

Oil and Fat Classification by FT-Raman Spectroscopy

Vincent Baeten,[†] Pierre Hourant,[‡] Maria T. Morales,[†] and Ramon Aparicio^{*†}

Instituto de la Grasa (CSIC), 4 Avenida Padre Garcia Tejero, 41012 Seville, Spain, and
Unité de Biochimie de la Nutrition, Catholic University of Louvain, Place Croix du Sud 2/bte 8,
1348 Louvain-la-Neuve, Belgium

One hundred and thirty-eight edible oil and fat samples from 21 different sources, either vegetable (Brazil nut, coconut, corn, high oleic sunflower, olive oil, peanut, palm, palm kernel, rapeseed, soybean, sunflower, etc.) or animal (butter, hydrogenated fish, and tallow) have been analyzed. The spectral features of the most noteworthy bands are studied, and their correlations with the amount of fatty acids quantified by gas chromatography are presented. Principal component analysis is applied to classify the set of samples by their level of unsaturation [saturated (SFA), monounsaturated (MUFA), and polyunsaturated fatty acids (PUFA)]. The most remarkable MUFA and PUFA oil sources are independently classified by applying stepwise linear discriminant analysis to the Raman shifts selected by their correlation with fatty acids or structural assignments. The results show that FT-Raman spectra not only have information of the degree of unsaturation but also of the balance among the amounts of SFA, MUFA, and PUFA. The scattering intensities near different Raman shifts (3013, 1663, and 1264 cm^{-1}) show high correlations with the fatty acid profile determined by gas chromatography.

Keywords: *Oils and fats; FT-Raman spectroscopy; chemometrics*

INTRODUCTION

Classical methods based on liquid or gas chromatography analysis are typically used to classify oils and fats. With the application of the Fourier transform algorithm to spectroscopy, Raman instruments have now the potential to substitute, or at least to complement, the classical methodologies for many control purposes.

The use of FT-Raman spectroscopy in food technology is supported by two basic contributions: the use of the Michelson interferometer and the use of near-infrared monochromatic light excitation (Diem, 1993). These contributions avoid the problems of classical dispersive Raman (fluorescence interference from the pigments, photodecomposition, wavelength calibration, lack of a precise frequency base from scan to scan, and difficulty to attain high-resolution spectra) without losing its traditional advantages (rapidity, no sample preparation or sample destruction, no use of unfriendly reagents, and suitability for on-line processes).

The good performances of the new generation of FT-Raman spectrometers regarding the signal-to-noise ratio, speed of analysis, and accuracy of wavelength calibration, together with the development of computer programs for data processing, have drastically increased its applications in food science (Li-Chan, 1996) as in other scientific fields (Gerrard and Birnie, 1992).

Traditionally, Raman scattering spectroscopy is presented versus mid-infrared absorption spectroscopy. In fact, these techniques are complementary and both are based on the discrete vibration transitions occurring in the ground electronic state of molecules. However,

Raman scattering arises from the change of polarizability or "shape" of the electron distribution in the molecule as it vibrates; in contrast, infrared absorption requires a change of the intrinsic dipole moment with the molecular vibration (Grasseli and Bulkin, 1991). Thus, infrared peaks are often broad, and this makes it difficult to find a peak that is completely free of the influence from an adjacent peak or from an external parameter (e.g., water vapor or CO_2). On the contrary, a Raman spectrum is frequently composed of a series of isolated bands and therefore the water and CO_2 have weak Raman scattering properties and produce few interferences. The second main difference is that the polar groups (such as $\text{C}=\text{O}$ and $\text{O}-\text{H}$) have strong infrared absorption bands, whereas nonpolar groups (such as $\text{C}=\text{C}$) show intense Raman scattering bands. In summary, these two branches of vibrational spectroscopy yield complementary information about molecular vibrations, each contributing to the spectral "fingerprint" of the molecules (Li-Chan, 1994).

The intensity of Raman bands depends on a few general rules: (i) nonpolar or slightly polar groups often give rise to stretching vibration of high Raman scattering intensity; (ii) Raman scattering bands from stretching vibrations are more intense than those from deformation vibrations; (iii) Raman scattering bands from symmetrical vibrations, which do not distort the molecule, have higher intensities than those from antisymmetric vibrations; (iv) the stretching vibrations of multiple bonds (e.g., $\text{C}=\text{C}$) often cause intense Raman scattering bands (Baranska et al., 1987; Grasseli and Bulkin, 1991).

However, there are some factors that modify the band positions (i.e., vibration frequencies). The most important are the interatomic distances, the spatial arrangement groups, the Fermi resonance, the physical state of the sample, the polarity of environment, the forma-

* Author to whom correspondence should be addressed (e-mail aparicio@cica.es).

[†] CSIC.

[‡] Catholic University of Louvain.

Table 1. Oil and Fat Samples (Number of Samples and Code of Each Source)

source	no. of samples	code	source	no. of samples	code
almond	1	a, ALM	rapeseed	13	m, RAP
Brazil nut	3	b, BNU	safflower	1	n, SAF
coconut	3	c, COC	sesame	1	o, SES
corn	10	d, COR	soybean	16	p, SOY
grape seed	2	e, GRA	sunflower	17	q, SUN
hazelnut	2	f, HAZ	high oleic SUN	7	g, HOS
walnut	1	h, NUT	margarine	2	r, MAR
olive oil	34	i, VOO	butter	2	s, BUT
peanut	11	j, PEA	hydrog fish	3	t, FIS
palm	3	k, PAL	tallow	3	v, TAL
palm kernel	3	l, PKO			

tion of hydrogen bonds, and the inductive, mesomeric, and field effects of neighboring groups (Baranska et al., 1987; Diem, 1993).

In this work, we illustrate the application of the new generation of Raman spectrometers (FT-Raman) in oil and fat classification. One hundred and thirty-eight edible oil and fat samples from 21 different sources (vegetable and animal sources) and species have been analyzed for their classification by the elucidation of the most noteworthy bands of their spectra. This paper analyzes not only the various levels of *cis* and *trans* isomers but also other structural information.

EXPERIMENTAL PROCEDURES

Sampling. A set of 138 commercial samples of the most representative oils and fats used in the food industry was analyzed (Table 1). A Belgian distributor supplied all of the oil and fat samples of coconut, high-oleic sunflower, hydrogenated fish, palm, palm kernel, and tallow, and six of each of the following vegetable oils: corn, peanut, rape, soybean, and sunflower. The rest of the samples of the latter group of seed oils plus other samples (safflower, walnut, grape seed, Brazil nut, almond, and sesame) were purchased from Belgian retailers and laboratories. Nineteen olive oil samples were also purchased in Belgium, and 15 virgin olive oil samples were chosen, from a set of 1428 (Aparicio and Alonso, 1994), with differing compositions in chemical compounds (triglycerides, alcohols, sterols, hydrocarbons, etc.). The hazelnut oils and the samples of butter and margarine were bought from local Spanish retailers.

Raman Analysis. All of the FT-Raman spectra were acquired on a Nicolet 910 FT-Raman spectrometer (Nicolet Analytical Instruments, Madison, WI) equipped with a nitrogen-cooled Ge detector that provided a superior signal-to-noise performance, allowing scanning time to be reduced. The 900 series houses a continuous wave Nd:YAG laser with an output at 1064 nm. The laser power is available from 0 to 1200 mW at the focus after filtering. In this work, however, an operating power of 500–540 mW provided the near-IR excitation.

Approximately 0.5 g of each sample was introduced into the glass tube. Fat samples were previously melted in a water bath at 40 °C before their insertion in the glass tube. FT-Raman spectra were obtained by placing each tube in front of the laser and focusing the Nd:YAG laser beam into the oil. All spectra were taken in the 180° backscattering refractive geometry and passed into the interferometer. Spectra were produced over the Raman shift 3250–0 cm⁻¹. Typically, 200 interferograms were co-added at 4 cm⁻¹ resolution with a sampling time of 4 min.

The glass cells were cleaned after each measure by aspirating the oil from the tube, washing twice with hexane, and wiping dry. The cleaned glass was checked spectrally to ensure that no residue of the previous sample or the solvent remained on the internal or external glass walls.

The spectrometer was coupled to a Nicolet 680D workstation under Nicolet software, version 3.20. Binary files of the

spectral data were accessible to personal computers through the NIC2DOS software. Spectra Calc software, version 2.2 (Galactic Industries Corp., St. Louis, MO) was used for spectra manipulation and transformation.

Chemical Analysis. Neutralization of the free fatty acids and alkaline methanolysis of the glycerides followed by esterification of the fatty acids was the procedure used (IUPAC, 1992). The organic phase was analyzed by a Carlo Erba (Milan, Italy) 600 Vega gas chromatograph equipped with an FID detector and a DP 800 integrator. Helium was used as the carrier gas. An BPX 70 capillary column (25 m × 0.2 mm i.d., 0.25 μm film thickness; Victoria, Australia) was used. An equal response factor was considered for the whole set of fatty acids.

Saturated (SFA), monounsaturated (MUFA), and polyunsaturated (PUFA) fatty acids were calculated from the pool of fatty acids quantified by gas chromatography (GC). The total unsaturation was calculated by the summation of the amount of unsaturated fatty acids (C16:1, C18:1, C18:2, and C18:3) quantified by GC.

Pre-treatment of Data. Savitsky–Golay nine-point smoothing function was applied over the range 3050–100 cm⁻¹ of each spectrum to reduce the noise affecting the spectral quality. This algorithm, the most familiar method of smoothing in analytical chemistry, is an indirect filter that fits the spectrum inside a wavenumber interval with a polynomial by the least-squares method. The parameters are the degree of the polynomial and the number of points to fit (Savitsky and Golay, 1964).

Univariate statistical algorithms of standard deviation and coefficient of variation (CV) were applied (i) to measure the quality of the analytical procedures, (ii) to select the regions of spectra that provide a good signal-to-noise ratio, and (iii) to carry out the calibration spectra.

The mathematical program removed the information concerning the baseline, as it is not relevant to this study, and retained the information of five regions: A, 3100–2805 cm⁻¹; B, 1770–1615 cm⁻¹; C, 1500–1420 cm⁻¹; D, 1345–1230 cm⁻¹; and E, 1150–850 cm⁻¹.

Each of these reduced spectra was normalized. All Raman scattering intensities were replaced by their normalized values using the standard deviation (SD) (standard score = (raw score – mean)/SD). This normalization drastically reduced the influences of the external variables. Fisher coefficient *F* (calculated as the ratio of the variance of samples between groups to within their group) was used to evaluate the mathematical normalization.

Factor analysis was applied under the general conditions of principal components analysis (PCA). The scree plot (Tabachnick and Fidell, 1983) was used for selecting the number of components retained. Later, a cross-validation repeated three times with different cancellation matrices always detected at least two significant components.

Stepwise linear discriminant analysis (SLDA) was applied to an initial set of Raman shifts (variables). The selection of these Raman shifts is explained throughout the text by their relation with structural assignments, according to the bibliography, or their correlation with the fatty acid composition of the samples. The variables are entered into (or removed from) the discriminant function according to the limits of *F*-to-enter and *F*-to-remove. *F*-distribution tables at *P* = 0.05 were used to fix the values for *F*-to-enter and *F*-to-remove to avoid good conclusions by chance. The set of samples was randomly divided into two separate groups, a test (70%) subset and a validation (30%) subset. The first subset is used to estimate the classification function, and the second subset is classified according to the function. By observing the proportion of correct classification for the second group, we have an empirical measure for the success of the discrimination or cross-validation with random subsamples.

The software was Excel 7.0 (Microsoft Corp.) and Statistica 6.0 (StatSoft, Tulsa, OK).

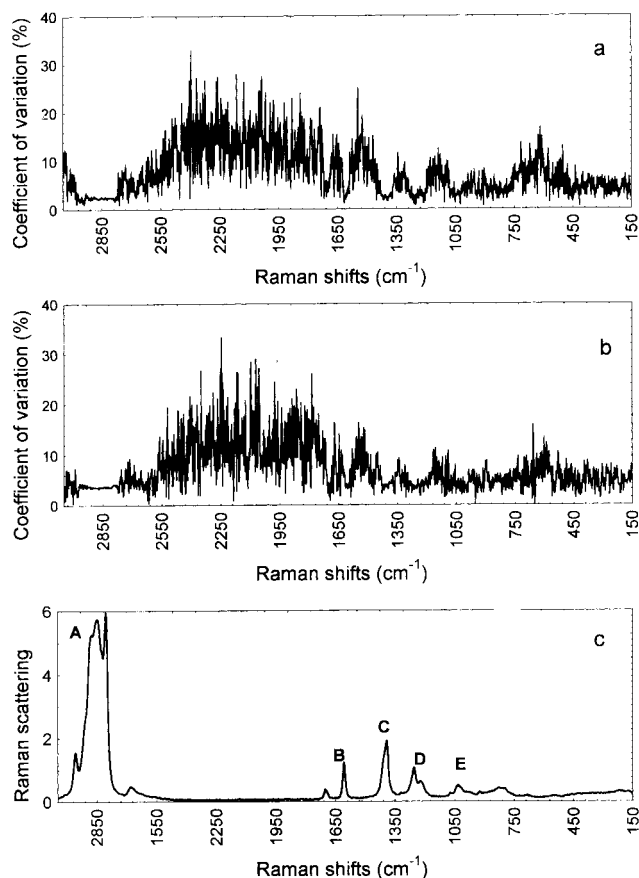


Figure 1. (a) CVs of an in-house common glass cell at each Raman shift; (b) CVs of an NMR glass cell at each Raman shift; (c) FT-Raman raw spectrum of an edible oil.

RESULTS AND DISCUSSION

Measurement of Performance: Uncertainty. On-line controls require that common glasses should be used but, theoretically, these glasses generate some loss in performance with respect to high-quality 5-mm NMR glass cells. The first study was to analyze the performance of in-house common glass cells and the uncertainty associated with these cells before the classification of oils and fats.

A set of 10 in-house glass cells was selected for the study after a visual inspection of their defects and a mathematical analysis of their signal-to-noise ratios. A repeatability study turning the cells 90° each time (four measures) was carried out with the selected cells.

Figure 1 displays the result of one of the selected in-house common glass cells (Figure 1a), in terms of coefficient of variation, versus an NMR glass cell (Figure 1b). The figures show that there are no significant differences between profiles of the CVs of NMR and in-house cells; in fact, the mean values of the CVs of the whole spectra were 7.2% for the NMR cell and 7.1% for the in-house cell. The maximum values of the CV correspond to the baseline, whereas the minimum values correspond to the Raman shifts of the regions A–E of the spectrum (Figure 1c). This region shows the most relevant information about the type of vibration of certain groups of atoms (Sadeghi-Jorabchi et al., 1990).

Once no statistically significant differences, in terms of repeatability, were found between the kinds of cells, the next steps were (i) to select the best four in-house

common glass cells for the final study of oils and fats classification and (ii) to establish the time in which the operating power supply was the most stable.

Table 2 shows the mean and the CV of each of the selected regions of the spectrum (A–E) for different experiments. The CVs of the four in-house glass cells were markedly lower than the high-quality NMR, although in-house cells showed a certain loss of information (lower mean) that could be evaluated at ~15%.

The best period of time for the measurements was delimited by analyzing an olive oil sample every 7 min up to 180 min. With the help of the statistical procedure of cluster analysis, it was detected that the laser power needed a period of stabilization of 35 min. The best repeatability, the most homogeneous results, was detected between 35 and 140 min. This study was carried out with the in-house cell numbered three, and its mean and CVs, for each selected region of the spectrum, appear in Table 2. This period of time was selected for the following experiments, although it can be prolonged by cooling the source and starting a new series of 140 min with 35 min of stabilization.

Table 2 also shows the repeatability study on seven different dates. This study provides the maximum error that can be associated with the measures. The CV of the spectra varied between 17.42 and 19.06% (repeatability A), which represents a great variation. However, when the normalization described previously to the repeatability study was applied, these figures did not go above 2.65%, indicating the accuracy of the data pretreatment. All of the spectra were normalized.

Detailed Analysis of the Most Noteworthy Spectral Regions. The FT-Raman spectrum of a virgin olive oil, displayed in Figure 1c, presents a series of bands with various Raman scattering intensities and shapes. Some regions of the spectrum (A–D) show a good signal-to-noise ratio and correspond to different types of vibration (ν , stretching; and δ , bending) of various groups of atoms (Sadeghi-Jorabchi et al., 1990). Unfortunately, a detailed and exhaustive description of the Raman scattered bands of an edible oil has not been published yet. Only some books (Baranska et al., 1987; Grasselli and Bulkin, 1991) and a few papers (Bailey and Horvat, 1972; Sadeghi-Jorabchi et al., 1990, 1991; Lerner et al., 1992; Li-Chan et al., 1994; Chmielarz et al., 1995; Baeten et al., 1996) describe the assignment to the major scattered bands of the FT-Raman spectrum of an edible oil (Table 3).

Region A (3100–2800 cm^{-1}) of the Raman spectra presents various scattered bands in the vicinity of different Raman shifts: 2965, 2935, 2895, and 2855 cm^{-1} . They are characteristics of the symmetric and antisymmetric $\nu(\text{C}-\text{H})$ vibration of the terminal chains of methyl (CH_3) and methylene (CH_2) groups of aliphatic molecules, which are the most abundant in edible oils and fats. These groups are significantly shifted if the methyl and methylene groups are linked to a carbon atom of an unsaturated group, or a heteroatom, instead of an aliphatic carbon atom (Baranska et al., 1987).

On the other hand, this region also contains a characteristic zone between 3020 and 2990 cm^{-1} , that is, Raman shifts near 3010 cm^{-1} resulting from the $\nu(=\text{C}-\text{H})$ vibration of methyl linoleate group (cis, cis diene) of olefinic molecules ($\text{RCH}=\text{CHR}$), 3006 cm^{-1} resulting from methyl oleate, and 3013 cm^{-1} of methyl linolenate (Sadeghi-Jorabchi et al., 1991). The Raman shift in the vicinity of 3010 cm^{-1} has been described as

Table 2. Means and CVs of the Selected Regions of the Spectrum (A–E) for Different Experiments^a

expt	zone of the spectrum									
	A		B		C		D		E	
	mean	CV	mean	CV	mean	CV	mean	CV	mean	CV
NMR cell	2.43	3.91	0.33	5.82	0.91	4.31	0.54	4.04	0.25	5.31
in-house cell										
1	2.04	2.17	0.29	4.20	0.77	1.29	0.47	2.43	0.26	3.40
2	2.40	1.22	0.28	2.21	0.77	1.03	0.47	1.04	0.24	1.97
3	2.05	2.53	0.28	4.61	0.77	2.15	0.47	2.87	0.25	3.78
4	2.04	1.09	0.29	2.10	0.77	0.98	0.47	1.22	0.26	1.70
time of work	1.96	2.55	0.32	3.99	0.76	2.51	0.47	2.70	0.26	3.87
repeatability A	2.01	17.69	0.29	18.42	0.76	19.06	0.46	18.62	0.26	17.42
repeatability B	2.07	0.16	0.27	1.52	0.77	1.99	0.46	2.65	0.25	1.80

^a Comparison between a high-quality NMR and four in-house glass cells. Statistical results for the period of time in which the operating power supply was more stable, the time of work. Repeatability study of the spectrum before (A) and after (B) the normalization.

Table 3. Assignments of the Major Raman Scattered Bands of an Edible Oil Spectrum

region	Raman shift (cm ⁻¹)	molecule	group	vibration ^a
A	3015	RCH=CHR	=C–H	ν asymmetric
	2970	–CH ₃	C–H	ν asymmetric
	2940	–CH ₂	C–H	ν asymmetric
	2900	–CH ₃	C–H	ν symmetric
	2860	–CH ₂	C–H	ν symmetric
B	1750	RC=OOR	C=O	ν
	1670	<i>trans</i> RCH=CHR	C=C	ν
	1660	<i>cis</i> RCH=CHR	C=C	ν
C	1445	–CH ₂	C–H	δ
D	1310	–CH ₂	C–H	δ
	1275	<i>cis</i> RCH=CHR	=C–H	δ
E	1100–1000	–(CH ₂) _n –	C–C	ν
	900–800	–(CH ₂) _n –	C–C	ν

^a ν , stretching; δ , deformation.

a useful indicator of the different degrees of unsaturation (Li-Chan et al., 1994), and it is correlated with the iodine value (Lerner et al., 1992). It has also successfully been used, together with other Raman shifts, in the detection and quantification of olive oil adulteration (Aparicio et al., 1996; Baeten et al., 1996).

Figure 2 shows the Raman scattered band near 3010 cm⁻¹ of various edible oils and fats. Each spectrum displayed in this figure—and the following ones—is the average of all the samples of each group of fats or oils. This figure shows that classifying the spectra is possible according to the Raman scattering intensity or according to the Raman shift (wavenumber) of their peaks. From high to low Raman scattering intensities (Table 4), the order is as follows:

(NUT, SAF, GRA) > (SUN, SOY, COR) >
 (RAP, SES) > (ALM, PEA, HAZ, BNU, MAR) >
 (HOS, VOO) > (PAL, TAL, FIS, BUT) >
 (PKO, COC)

Moreover, the intensities near 3013 cm⁻¹ agree ($R^2 = 0.94$) with the degree of unsaturation described by the equation (GC amount of C18:1) + 2(GC amount of C18:2) + 3(GC amount of C18:3). This equation is derived from an AOCS standard (AOCS, 1997) after the minor fatty acids (C16:1, C20:1, C22:1) have been removed and normalizing it by 0.860.

On the other hand, the order of Raman shifts (cm⁻¹), from high to low

(NUT)₃₀₁₉ > (SAF, GRA, SUN, SOY, COR, RAP, PEA, SES, MAR, BNU)₃₀₁₇ >
 (ALM, HAZ, PAL)₃₀₁₅ >
 (HOS, VOO, TAL, PKO, COC)₃₀₁₃ >
 (BUT)₃₀₁₁ > (FIS)₃₀₀₈

can be explained by the types of fats and oils clustered inside three great groups: (i) the samples with a high content of PUFA; (ii) the samples with a high content of MUFA; and (iii) the fats that have a high content of SFA. The scattering intensities near 3015 cm⁻¹ are highly correlated ($R^2 = 0.93$) with the amount of PUFA determined by GC (C18:2 + C18:3).

Other Raman shifts of this region have also typical features; for example, the order of samples near 2857 cm⁻¹ can be explained by their degree of saturation. The samples with a high degree of SFA have a higher intensity at this band as saturated oils and fats have many methylene chain and methyl terminal chain groups.

Region B (1800–1600 cm⁻¹) shows two main bands near 1750 and 1660 cm⁻¹. The first band (not shown) corresponds to the relatively weak carbonyl bond ν -(C=O) scattered band. This band is shifted to lower Raman shifts for methyl ester compounds in comparison with the position for triglyceride compounds (Bailey and Horvat, 1972). This band, in the vicinity of 1750 cm⁻¹, showed very little useful information. Only samples with a high content of saturated and short fatty acids (palm kernel, palm, coconut, . . .) showed a relatively high Raman scattering intensity.

The second part of this region is richer in variations and useful information (Figure 3). The band surrounding 1660 cm⁻¹ is characteristic of the ν (C=C) vibration of olefinic molecules. This region shows a strong scattered band over the Raman shift range of 1670–1650 cm⁻¹ since many different factors have an influence on this band. In fact, if the C=C bond is conjugated with another double bond, then the stretching frequency is shifted 30–50 cm⁻¹ toward lower frequencies because this band is sensitive to the number of double bonds. Moreover, the spatial configuration of the conjugated system can also influence the Raman shifts.

Bailey and Horvat (1972) stated that the frequency shifts and bandwidths of the C=C bond from pure methyl ester and triglyceride compounds vary according to the relation between the *cis* (1656 cm⁻¹) and *trans*

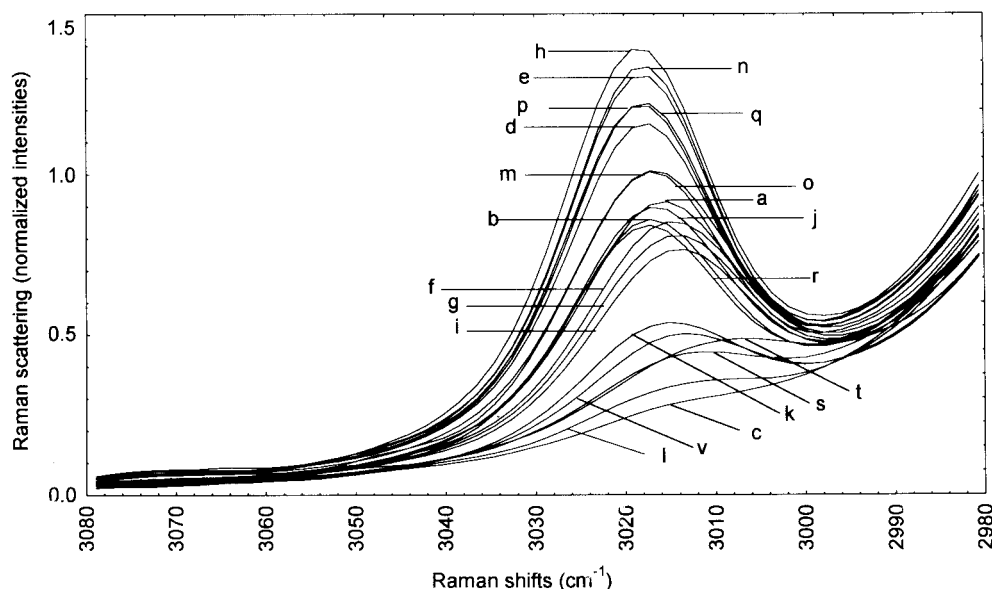


Figure 2. Mean of the Raman spectra of edible fat and oil samples: region A, Raman shifts 3080–2980 cm^{-1} . Codes are described in Table 1.

Table 4. Mean of Raman Scattering Intensities (after Normalization) at Four Raman Shifts for Each of the Oil and Fat Sources^a

code	variety	3010 cm^{-1}	1660 cm^{-1}	1300 cm^{-1}	1265 cm^{-1}	SFA	MUFA	PUFA
a	ALM	0.84	0.73	0.38	0.31	8.4	70.3	21.2
b	BNU	0.74	0.57	0.35	0.27	28.9	35.2	35.9
c	COC	0.30	0.04	0.31	0.09	92.2	16.2	1.6
d	COR	0.94	0.83	0.38	0.39	13.8	26.4	59.8
e	GRA	1.01	0.97	0.40	0.44	13.1	18.3	68.6
f	HAZ	0.83	0.76	0.41	0.31	9.9	74.0	16.1
g	HOS	0.78	0.64	0.40	0.28	8.7	79.3	12.0
h	NUT	1.06	1.04	0.40	0.48	9.6	17.8	72.6
i	VOO	0.74	0.58	0.38	0.24	15.0	76.3	8.7
j	PEA	0.79	0.68	0.38	0.30	15.1	44.0	40.9
k	PAL	0.52	0.32	0.35	0.17	53.2	35.8	11.0
l	PKO	0.35	0.10	0.32	0.10	85.0	11.5	3.5
m	RAP	0.89	0.87	0.38	0.39	7.3	59.7	33.0
n	SAF	1.03	0.97	0.38	0.44	7.2	15.7	77.1
o	SES	0.87	0.72	0.37	0.32	12.1	42.0	45.9
p	SOY	0.97	0.87	0.38	0.39	16.2	21.7	62.1
q	SUN	0.97	0.90	0.39	0.40	10.9	22.3	66.8
r	MAR	0.72	0.64	0.41	0.29	31.8	39.2	29.0
s	BUT	0.45	0.29	0.40	0.15	64.8	29.8	5.4
t	FIS	0.47	0.18	0.39	0.13	55.2	40.0	4.8
v	TAL	0.50	0.31	0.35	0.15	54.8	40.6	4.6

^a Percentages of SFA, MUFA, and PUFA quantified by GC.

(1670 cm^{-1}) isomers' content and from single to double bonds. These authors also observed that the fraction of the total C=C stretch scattering is directly proportional to the trans isomer fraction. They established that the ratio of $\nu(\text{C}=\text{C})_{(1691-1626 \text{ cm}^{-1})}$ to $\delta(\text{CH}_2)_{(1476-1420 \text{ cm}^{-1})}$ is inversely correlated with the content of SFA. Sadeghi-Jorabchi et al. (1990) used this ratio to determine the iodine value in margarines. The correlation between the $\nu(\text{C}=\text{C})$ and the iodine value has also been studied in cooking oil (Lerner et al., 1992). It was used to determine the total content of cis and trans isomers in linseed oil (Chmielarz et al., 1995). Bailey and Horvat (1972) also stated that the isolated and conjugated isomers can be distinguished by a small difference in the position of the C=C double bond: isolated double stretch above 1650 cm^{-1} , conjugated dienes about 1630 cm^{-1} , and conjugated trienes below 1630 cm^{-1} . The Raman shift near 1660 cm^{-1} has also been used in virgin olive oil authentication. Baeten et al. (1996) have shown

that this band is correlated with the content of trilinolein ($R^2 > 0.87$), so offering promising results in the detection of virgin olive oil adulteration at low percentages (Baeten and Aparicio, 1997).

Figure 3 shows the spectra of oils and fats in the vicinity of 1660 cm^{-1} . The decreasing values of the Raman scattering intensities in this region (Table 4) show the order

(NUT, SAF, GRA) > (SUN, SOY, COR) >
 (SES, ALM, HAZ, RAP, PEA, MAR) >
 (BNU, HOS, VOO) > (PAL, TAL, BUT) >
 (PKO, FIS, COC)

which can be explained by the degree of unsaturation of these sources. A good correlation has been obtained ($R^2 = 0.93$) between the Raman intensities, near 1663 cm^{-1} , and the total unsaturation. Following now the X-axis, from left to right, the fats and oils appear clustered into three groups:

(FIS)₁₆₇₅ >
 (NUT, SAF, GRA, SUN, SOY, COR, SES,
 ALM, RAP, PEA, BNU, MAR)₁₆₆₃ >
 (HAZ, HOS, VOO, PAL, TAL, BUT, PKO, COC)₁₆₆₁

Near 1670 cm^{-1} , the Raman scattering intensity is higher for the hydrogenated fish oil samples, so revealing their high content of trans fatty acids. These samples also show a shoulder in the area of 1660 cm^{-1} that attests to the presence of cis isomers. This observation is confirmed by chromatographic results. For samples presenting bands near 1661 or 1663 cm^{-1} , the slight shift to the lowest frequencies corresponds to samples with a high level of PUFA. The Raman shift near 1665 cm^{-1} is highly correlated ($R^2 = 0.93$) with the amount of PUFA determined by GC.

Region C (1600–1390 cm^{-1}) shows a single scattered band near 1440–1445 cm^{-1} (not displayed) that corresponds to the $\delta(\text{C}-\text{H})$ deformation vibration. This band has been used by various authors in the determination of the total unsaturation (Bailey and Horvat, 1972;

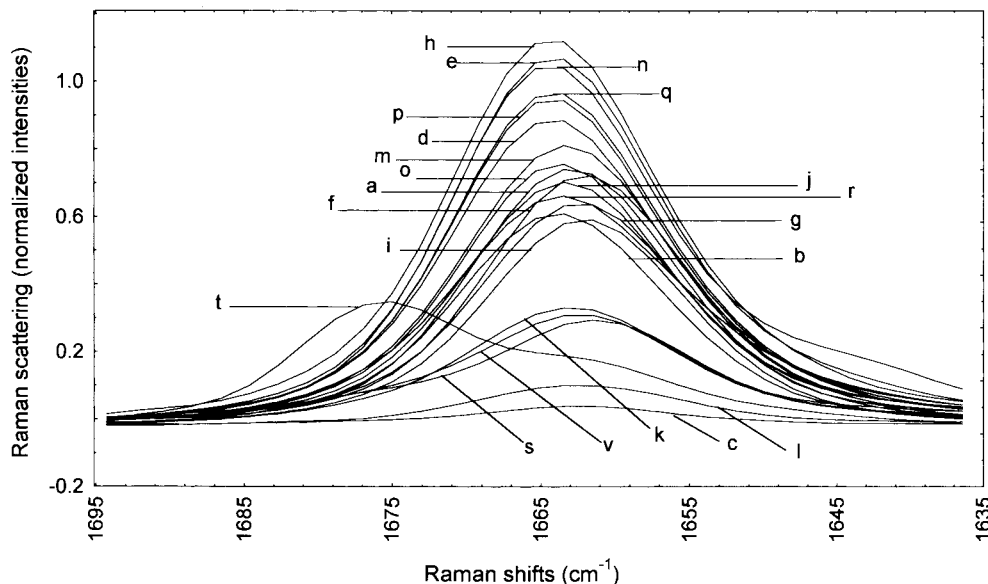


Figure 3. Mean of the Raman spectra of edible fat and oil samples: region B, Raman shifts 1695–1635 cm^{-1} . Codes are described in Table 1.

Sadeghi-Jorabchi et al., 1990), but we have been unable to find a good correlation ($R^2 < 0.4$). However, it has been successfully used in the detection of virgin olive oil adulteration (Baeten et al., 1996).

Region D (1390–1200 cm^{-1}) has two bands centered near 1303 and 1270 cm^{-1} . The band in the vicinity of 1303 cm^{-1} corresponds to in-phase methylene twisting deformation vibration, whereas the second band corresponds to the in-plane $=\text{C}-\text{H}$ deformation vibration of unconjugated cis double bonds. Sadeghi-Jorabchi et al. (1991) detected cis monoene, diene, and triene isomers, respectively, near 1267, 1265, and 1266 cm^{-1} , whereas no absorption of the trans isomer double bond was detected in the vicinity of these bands. These results indicate that the band near 1265 cm^{-1} estimates the levels of cis unsaturation without any interference from the trans isomer. Recently, Li-Chan (1996) reported that the total cis isomer content can be determined from the ratio between the Raman intensities around 1265 and 1303 cm^{-1} . This ratio showed an excellent correlation with the results from GC analysis (Sadeghi-Jorabchi et al., 1991). Baeten et al. (1996) used the band at 1265 cm^{-1} in the authentication of olive oil. In the present study, the wavenumber in the vicinity of 1264 cm^{-1} has been correlated ($R^2 = 0.93$) with the total amount of unsaturation determined by GC. Furthermore, this region contains a band near 1320 cm^{-1} that corresponds to the trans isomer double bond (Lerner et al., 1992).

Region E (1200–700 cm^{-1}) shows the spectral features present in the final part of the Raman spectrum, the so-called fingerprint. This region contains bands that are characteristics of C–C skeletal and C–O bond vibrations. Bands arising from $\nu(\text{C}-\text{C})$ vibration were unable to distinguish the samples and are therefore useless as an additional piece of information for the identification of the carbon chain.

The hydrocarbon chains are characterized by a series of bands (three or four) due to the vibration of skeletal C–C bonds in the ranges 1100–1000 and 900–800 cm^{-1} , whereas C–O bonds have characteristic features in two bands near 1150–1060 and 970–800 cm^{-1}

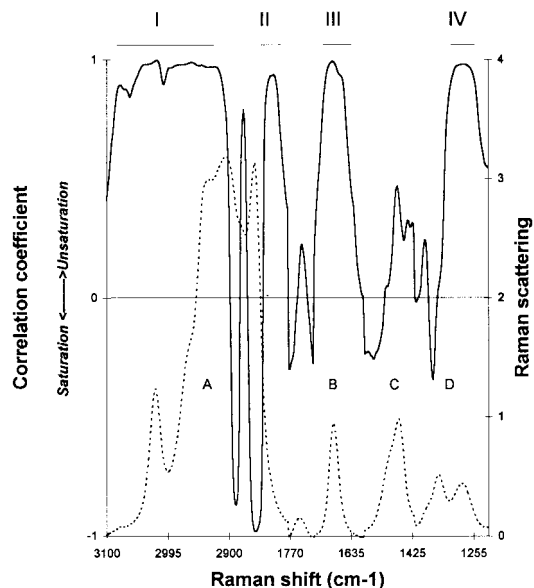


Figure 4. Values of the correlation coefficients between Raman scattering intensities and the total unsaturation at each Raman shift. The dotted line is the FT-Raman spectrum of the selected regions

(Baranska et al., 1987). The carbon chain deformation vibration has also been detected in the area 450–150 cm^{-1} .

In our study, the spectra show some bands (near 1125, 1085, 980, and 875 cm^{-1}) that could characterize the samples of oils and fats. The high signal-to-noise ratio and the influence of some external phenomena (e.g., lattice effect) dramatically diminish the potential usefulness of this region for quantitative and qualitative analysis.

The spectral study of all the samples shows that their Raman spectra mainly contain information about the unsaturated (MUFA and PUFA) fatty acids. Figure 4 displays the correlation coefficient—at each Raman shift—between the Raman scattering intensities and the total unsaturation [measured as the amount of unsaturated fatty acids (C16:1, C18:1, C18:2, and C18:3) quantified by GC]. The figure clearly shows four

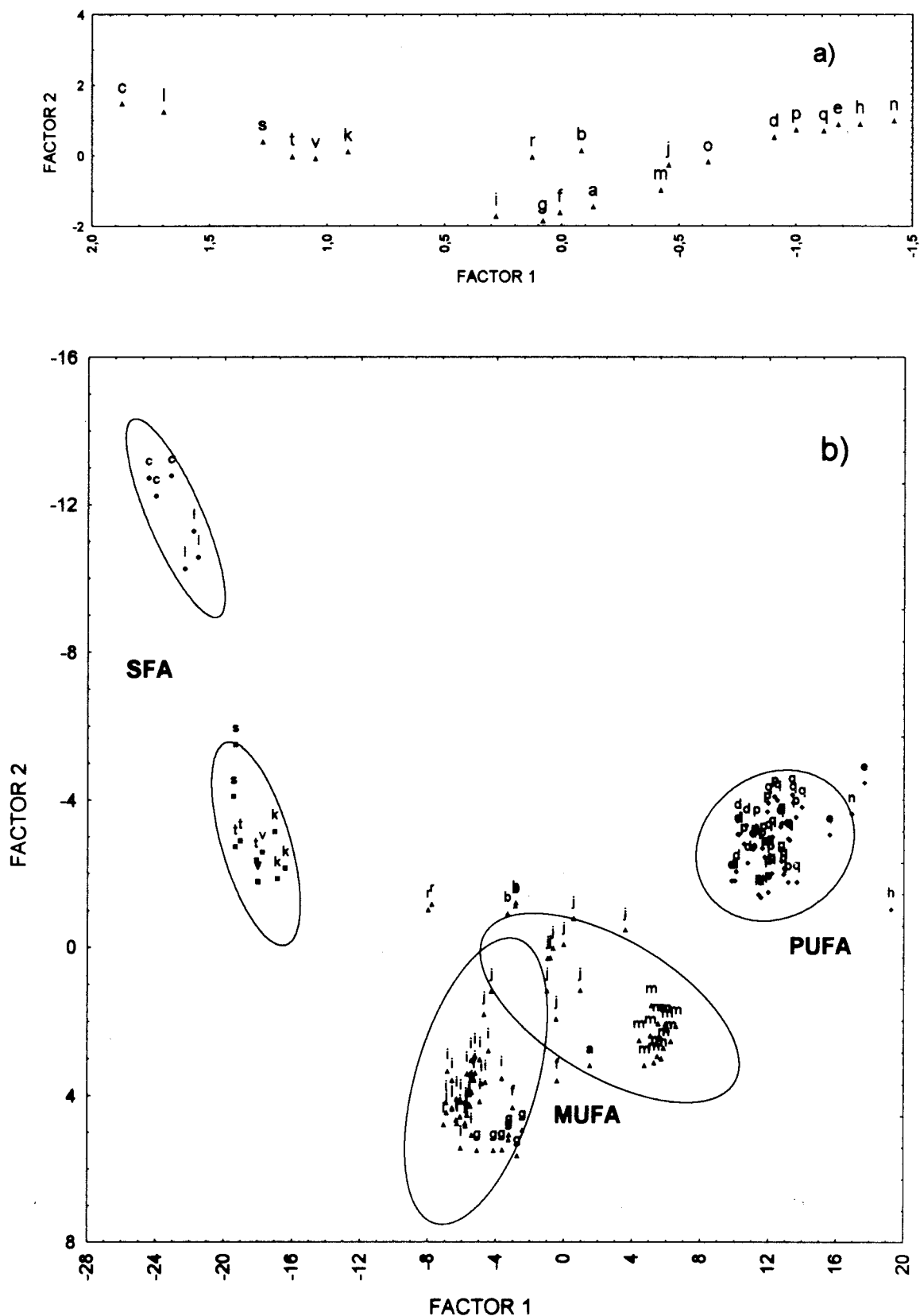


Figure 5. PCA of fatty acids calculated by GC (a) and selected Raman shifts. Ellipses represent the 95% confidence regions of the basic groups described by fatty acids (b). Codes are described in Table 1.

spectral regions (I–II, III, IV) where the correlation coefficients are $>90\%$. Bands I, III, and IV are related to the double-bond vibration (stretching and bending) of the olefinic chain. The spectral band between 2900 and 2850 cm^{-1} is negatively correlated with the amount

of total unsaturation. This region is related to the amount of C–H bond vibration of CH_2 and CH_3 groups and therefore contains more information about the SFA.

Figure 5a shows the result of applying PCA to the mean values of fatty acids quantified by GC. The oils

and fats appear clustered into the three types of unsaturation, SFA, MUFA, and PUFA.

Factor 1 (55.2% of the explained variance) is positively correlated with SFA and negatively with PUFA. Factor 2 (44.8% of the explained variance) is negatively correlated with MUFA. Thus, from left to right, the level of unsaturation goes from saturated (SFA) to polyunsaturated (PUFA), the monounsaturated fatty acids (MUFA) being in the middle. The group of SFA clusters two subgroups, coconut (c) and palm kernel (l), as the most saturated fats, and a second group that clusters less saturated fats and oils: butter (s), hydrogenated fish (t) fats, tallow (v), and palm (k) fats.

The oils and fats with MUFA are clustered into three great groups: the most monounsaturated includes olive (i), high-oleic sunflower (g), hazelnut (f), and almond (a) oils; a little less monounsaturated includes margarine (r) and Brazil nut (b) oils; and monounsaturated but with a certain level of polyunsaturation includes peanut (j), rapeseed (m), and sesame (o) oils.

The oils with PUFA are clustered into a single group, although with a progressive level of polyunsaturation. The hypothetical line of polyunsaturation starts with corn (d) and soybean (p) oils and ends with safflower (n) oil.

Figure 5b shows the results of FT-Raman. PCA was applied to that set of Raman shifts correlated with certain structural assignments (Sadeghi-Jorabchi et al., 1990) or with the fatty acids quantified by GC.

Factor 1 (explaining 74.96% of the total variance) is made up almost exclusively of the Raman shifts 3013, 3010, 3006, 2965, 2935, 1670, 1665, 1663, and 1660 cm^{-1} . Factor 2 (explaining 13.69% of the total variance) is made up of two Raman shifts, 2895 and 2855 cm^{-1} . The ellipses show the 95% confidence regions for each of the groups described in Figure 5a. These ellipses allow an interpretation beyond the simple location of samples:

(i) The groups of SFA (Figure 5a) completely agree with those obtained using FT-Raman. Therefore, the most saturated oils and fats [coconut (c) and palm kernel (l)] appear quite separate from the less saturated oils and fats. In fact, coconut and palm kernel have closely related chemical compositions as both contain $\sim 47\%$ lauric acid and have low levels of unsaturation.

(ii) The two groups with high MUFA, detected by GC, also appear in the information of FT-Raman. There is only a small difference. The peanut (j) samples appear closer to olive oils than rapeseed oils (m) using the information of FT-Raman. Figure 6a shows that peanut (j), olive oil (i), high-oleic sunflower (g), rapeseed (m), hazelnut (f), and Brazil nut (b) oils can be classified by two profiles of the Raman shifts 3020, 3006, 2965, 2857, 1656, 1650, and 1267 cm^{-1} . These profiles were obtained using SLDA under the conditions described under Mathematical Analysis.

(iii) PUFA oils are so close that is almost impossible to distinguish one from the other; for example, corn oil has a fatty acid composition that overlaps the other oils (Aparicio, 1997). Similar results were pointed out by FT-Raman when PCA was applied, but SLDA was able to build two profiles that can distinguish the most remarkable vegetable oils (COR, SOY, and SUN; Figure 6b). The profiles are based on the Raman shifts 2935, 2855, 1661, 1630, and 1303 cm^{-1} .

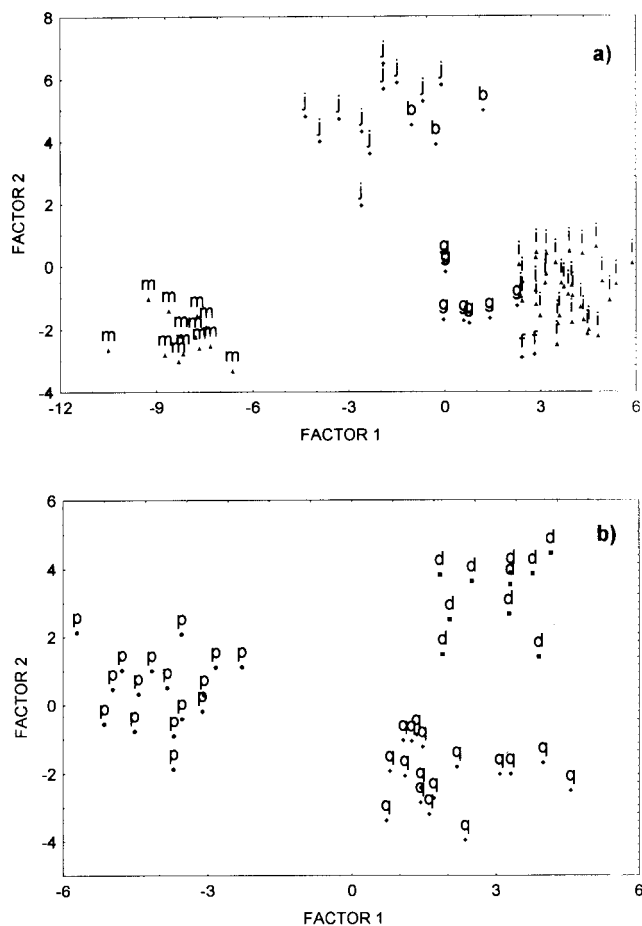


Figure 6. SLDA of monounsaturated (a) and polyunsaturated (b) oils. Codes are described in Table 1.

The results show that FT-Raman can classify edible oils and fats according to their degree of unsaturation on the basis of a few wavenumbers (Figure 5b). Some of these wavenumbers are related to the unsaturations measured by GC, pointing out that they were not selected at random when statistical procedures were applied. However, this is a basic classification that can be used as the root of an arborescent structure in which the branches are SFA, MUFA, and PUFA groups. Analyzing the MUFA hypothetical branch, the statistical procedure was able to distinguish between the edible oils [plus margarine (r)] clustered inside MUFA by the first classification. Figure 6a shows that factor 2 determines two great groups composed by edible oils with a ratio between MUFA and PUFA ~ 1 [Brazil nut (b), 0.98; peanut (j), 1.08, upper part of the figure] against those with ratio > 1 (lower part of the figure). Factor 1 classifies the edible oils of this second group according to the empirical value of that ratio: rapeseed oil (m; 1.8), high-oleic sunflower oil (g; 2.4), hazelnut oil (f; 6.6), and olive oil (i; 8.8), the three latter oils being clustered inside the fourth quadrant of the plot. The mathematical procedures selected those wavenumbers to explain the vibrations related to double bonds ($\text{C}=\text{H}$ and $\text{HC}=\text{CH}$).

The classification of edible oils inside the PUFA group was carried out by wavenumbers mostly explaining the fatty acid chain ($\text{C}-\text{H}$) and cis double bonds ($\text{HC}=\text{CH}$). FT-Raman had more problems in classifying the edible oils [soybean (p), corn (d), and sunflower (q) oils] into clear separate groups (Figure 6b). Factor 1 shows two great groups that can be explained by the amount of

linolenic acid (C18:3)/soybean oil (6.7–8.3%) versus sunflower oil (0.1–0.3%) and corn oil (0.6–1.1%). The total content of PUFA can by and large explain the differences between corn and sunflower oils in the plot. The total content of PUFA (C18:2 + C18:3) of soybean oil (60.3–63.2%) is between that of corn oil (57.1–61.3%) and that of sunflower oil (64.9–67.9%).

This basic arborescent structure can be used to characterize edible oils and keep their spectra at nodes of an expert system (Aparicio, 1988). The synergy of spectroscopic techniques and artificial intelligence procedures has already been used with success in different aspects of food sciences (Zupan et al., 1988; Aparicio, 1997).

ACKNOWLEDGMENT

We express our indebtedness to Drs. Ángel Justo and Miguel Angel Avilés of the Instituto de Ciencias de los Materiales (CSIC, Seville, Spain) for solving many experimental problems and allowing us to use the FT-Raman spectrometer and to Drs. Debruyne and Breemeersch of S.A. Vandemoortele (Belgium) for purchasing some of the samples used in this study.

LITERATURE CITED

- American Oil Chemists' Society. Recommended practice Cd 1c-85, Calculated iodine value; AOCS: Champaign, IL, 1997.
- Aparicio, R. Characterization of foods by inexact rules: the SEXIA expert system. *J. Chemom.* **1988**, *3*, 175–192.
- Aparicio, R. Results of fats and oils commodity group of the Research Project Food Authenticity: Issues and Methodologies. Presented at the 4th European Symposium on Food Authenticity; La Baule, France, June 1997.
- Aparicio, R.; Alonso, V. Characterization of virgin olive oils by SEXIA expert system. *Prog. Lipid Res.* **1994**, *33*, 29–38.
- Aparicio, R.; Morales, M. T.; Baeten, V. Detection of virgin olive oil adulteration by FT-Raman spectroscopy. Presented at the 87th American Oil Chemists' Society Annual Meeting, Indianapolis, IN, 1996.
- Baeten, V.; Aparicio, R. Possibilities offered by infrared and Raman spectroscopic techniques in Virgin olive oil authentication. *Olivae* **1997**, *69*, 38–43.
- Baeten, V.; Meurens, M.; Morales M. T.; Aparicio, R. Detection of virgin olive oil by Fourier transform Raman spectroscopy. *J. Agric. Food Chem.* **1996**, *44*, 2225–2230.
- Bailey, G. F.; Horvat, R. J. Raman spectroscopy analysis of the cis/trans isomer composition of edible vegetable oils. *J. Am. Oil Chem. Soc.* **1972**, *49*, 494–498.
- Baranska, H.; Labudzinska, A.; Terpinski, J. *Laser Raman Spectrometry: Analytical Applications*; Ellis Horwood: Chichester, U.K., 1987.
- Chmielarz, B.; Bajdor, K.; Labudzinska, A.; Klukowska-Majewska, Z. Studies on the double bond positional isomerization process in linseed oil by UV, IR and Raman spectroscopy. *J. Mol. Struct.* **1995**, *348*, 313–316.
- Diem, M. *Introduction to Modern Vibrational Spectroscopy*; Wiley: New York, 1993.
- Gerrard, D. L.; Birnie, J. Raman spectroscopy. *Anal. Chem.* **1992**, *64*, 502R–513R.
- Grasseli, J. G.; Bulkin, B. J. *Analytical Raman Spectroscopy*; Wiley: New York, 1991.
- IUPAC (International Union of Pure and Applied Chemistry). *Standard Methods for the Analysis of Oils, Fats and Derivatives*, 1st supplement, 7th ed.; Dieffenbacher, A., Pocklington, W. D., Eds.; Blackwell Scientific Publication: Oxford, U.K., 1992; Method 2.301.
- Lerner, B.; Garry, M.; Walder, F. Characterization of polyunsaturation in cooking oils by the 910 FT-Raman. *Proceedings of the 2nd International on FT-IR*; Vansant, E. F., Ed.; University of Antwerp: Antwerp, Belgium, 1992; pp 75–82.
- Li-Chan, E. C. Y. Developments in the detection of adulteration of olive oil. *Trends Food Sci. Technol.* **1994**, *5*, 3–11.
- Li-Chan, E. C. Y. The application of Raman spectroscopy in food science. *Trends Food Sci. Technol.* **1996**, *7*, 361–370.
- Martens, H.; Naes, T. *Multivariate Calibration*; Wiley: Chichester, U.K., 1989.
- Sadeghi-Jorabchi, H.; Hendra, P. J.; Wilson, R. H.; Belton, P. S. Determination of the Total Unsaturation in Oils and Margarines by Fourier Transform Raman Spectroscopy. *J. Am. Oil Chem. Soc.* **1990**, *67*, 483–486.
- Sadeghi-Jorabchi, H.; Wilson, R. H.; Belton, P. S.; Edwards-Webb, J. D.; Coxon, D. T. Quantitative analysis of oils and fats by Fourier transform Raman spectroscopy. *Spectrochim. Acta* **1991**, *47A* (9/10), 1449–1458.
- Savitsky, A.; Golay, M. J. E. Smoothing and differentiation of data by simplified least-squares procedures. *Anal. Chem.* **1964**, *36* (8), 1627–1630.
- Tabachnick, B. G.; Fidell, L. S. *Using Multivariate Statistics*; Harper & Row: New York, 1983.
- Zupan, J.; Razinger, M.; Bohanec, S.; Novic, M.; Tusar, M.; Lah, L. Building knowledge into an expert system. *Chemom. Intell. Syst.* **1988**, *4*, 307–314.

Received for review September 12, 1997. Revised manuscript received April 3, 1998. Accepted April 30, 1998. This work has partially been supported by the project EC FAIR-CT965053.

JF9707851